RSC Advances

PAPER

View Article Online
View Journal | View Issue

Cite this: *RSC Adv.*, 2020, **10**, 15171

Fabrication of magnetic iron oxide-supported copper oxide nanoparticles (Fe_3O_4/CuO): modified screen-printed electrode for electrochemical studies and detection of desipramine

Somayeh Tajik,*[ab] Hadi Beitollahi,[c] Mohammad Reza Aflatoonian,[bd] Bita Mohtat,[e] Behnaz Aflatoonian,[a] Iran Sheikh Shoaie,[f] Mohammad A. Khalilzadeh,[g] Marzieh Ziasistani,[f] Kaiqiang Zhang,[h] Ho Won Jang *[h] and Mohammadreza Shokouhimehr *[h]

The present investigation examines a sensitive electrochemical technique to detect desipramine through Fe_3O_4/CuO nanoparticles (NPs). Fe_3O_4/CuO NPs were synthesized *via* a coprecipitation procedure, and the products were characterized *via* energy disperse spectroscopy, X-ray diffraction, transmission electron microscopy, scanning electron microscopy, and vibrating sample magnetometer. The voltage–current curve and differential pulse voltammetry examinations of Fe_3O_4/CuO-modified screen-printed electrode (Fe_3O_4/CuO/SPE) were followed by the determination of electro-catalytic activities toward desipramine oxidation in a phosphate buffer solution (pH = 7.0). In addition, the value of diffusion coefficient ($D = 3.0 \times 10^{-6}$ cm^2 s^{-1}) for desipramine was calculated. Then, based on the optimum conditions, it was observed that the currents of the oxidation peak were linearly proportionate to the concentration of desipramine in the broad range between 0.08 and 400.0 μM and LOD of 0.03 μM (S/N = 3). Finally, our new sensor was successfully utilized to detect desipramine in the real samples, with reasonable recovery in the range of 97.2% to 102.7%.

Received 14th March 2020
Accepted 2nd April 2020

DOI: 10.1039/d0ra02380a

rsc.li/rsc-advances

Introduction

Currently, researchers have attempted to construct electrochemical sensors because they have properties such as selectivity, sensitivity, rapid responses, specificity, and simplified fabrication. In fact, electrochemical sensors contribute vitally to the medicine analyses.[1–7] In electrochemical analysis, the key component is electrode modification, which is one of the reasonable and robust strategies to resolve the limitations of the unmodified electrode, including lower selectivity, sensitivity, and stability as well as the blockade of electron transfer. Thus, experts in the field used diverse electroactive compositions to modify the surface.[8–15]

According to the studies, nano-technology is rapidly progressing towards the industrial applications in the areas of catalysts, isolation, synthesis, luminescence, and sensing.[16,17] Owing to their specific physicochemical features such as higher surface area and better sensitivity, nanomaterials have been considered for CL reactions as the catalyst, energy acceptor, enhancer, and platform of the CL resonance energy transfer.[18,19]

Current authors reported that nanoparticles (NPs) are largely involved in the quality of the sensing tools. According to the voltammetric examinations, they utilized such particles as the electrode modifiers to improve special surface areas, mass transport, and catalytic efficiency.[20–27]

Based on the investigations, the magnetic particles of the nano-metric size, particularly the iron oxide (Fe_3O_4) NPs, have been considered because of the respective super-paramagnetic characteristics; however, their utilization is restricted owing to the larger ratio of surface to volume and robust dipole–dipole attraction between the particles, as magnetic features of Fe_3O_4 are poor, and the functional groups are restricted for selective bindings. Of course, researchers applied substances such as metals and metal oxides to modify the Fe_3O_4 NP surface for

[a]*Neuroscience Research Center, Kerman University of Medical Sciences, Kerman, Iran. E-mail: tajik_s1365@yahoo.com*

[b]*Research Center for Tropical and Infectious Diseases, Kerman University of Medical Sciences, Kerman, Iran*

[c]*Environment Department, Institute of Science and High Technology and Environmental Sciences, Graduate University of Advanced Technology, Kerman, Iran*

[d]*Leishmaniasis Research Center, Kerman University of Medical Sciences, Kerman, Iran*

[e]*Department of Chemistry, Islamic Azad University, Karaj Branch, Karaj, Iran*

[f]*Department of Chemistry, Faculty of Science, ShahidBahonar University of Kerman, Kerman 76175-133, Iran*

[g]*Department of Forest Biomaterials, College of Natural Resources, North Carolina State University, Raleigh, North Carolina 27607, USA*

[h]*Department of Materials Science and Engineering, Research Institute of Advanced Materias, Seoul National University, Seoul 08826, Republic of Korea. E-mail: mrsh2@snu.ac.kr; hwjang@snu.ac.kr*

avoiding the self-aggregation and improving chemical stability. However, for their specific and reasonable features, researchers considerably attended the metal oxides NPs. In fact, Fe_3O_4/CuO NPs have a widespread utilization to modify the electrodes since they augment the electrical conductivity and electrodes surface. Moreover, they enhance the electron transfer kinetics between the surface of the electrode and a wider range of the electro-active samples.[28–32]

Researchers believe that SPEs are a very beneficial means to design disposable sensors for applying in the electro-analysis. Actually, SPEs are very flexible, can be easily used, are affordable analytical instruments, and finally are appropriate for miniaturization.[33–37] Thus, Au, Hg, and Bi films are used to coat SPEs for improving the respective electrochemical functions.

Some studies illustrated that tricyclic anti-depressants such as desipramine have a mechanism at the presynaptic level in obstructing the reuptake of the monoamines, in particular, dopamine, norepinephrine, and serotonin. It has also been found that the post-synaptic activities involve obstructing the muscarinic receptors (cholinergic), alpha-2, histamine type-1, beta-adrenergic, and anti-depressant effects. However, they suffer from some complications. In particular, the therapeutic range for desipramine lies between 115–250 ng mL^{-1}, whereas the toxic dose starts above 500 ng mL^{-1}, and the plasma half-life is 12–28 hours.[38] Numerous papers published correlation of the tricyclic anti-depressant overdose and severe body dysfunctions such as sleepiness, seizure, respiratory issues, and coma. Therefore, the medicine dose in the organism should be highly monitored.[39,40]

It is notable that the most utilized analytical procedures to detect desipramine relied on gas and liquid chromatography,[41,42] electrophoresis,[43] and spectrophotometry.[44] However, detecting desipramine *via* the above methods showed higher sensitivity. However, they require costly tools, laborious pretreatment phases, trained operators, and multiple organic solvents. In addition, it is not possible to use the mentioned procedures for *in situ* assays. In this way, the methodologies using the electrochemical techniques are interesting because of their rapidness, good sensitivity, and selectivity.[45–48]

Herein, the procurement and utilization of a novel Fe_3O_4/CuO/SPE for the determination of desipramine are described. Under optimum conditions, it was found that the modified electrode had higher sensitivity, lower LOD, and wider linear dynamic range compared to the bare electrode. Moreover, the analytical applicability of the modified sensor in quantifying desipramine in the real samples was evaluated with satisfactory results.

Experimental

Chemicals and apparatus

We conducted the electrochemical tests using an Autolab potentiostat/galvanostat (PGSTAT 302N, Eco Chemie: the Netherlands), and then, we monitored the system by a general-purpose electrochemical system software.

It should be noted that SPE (DropSens: DRP-110, Spain) has 3 traditional electrodes called the graphite counter electrode, an unmodified graphite working electrode, and a silver pseudo-reference electrode. Moreover, we used a Metrohm 710 pH-meter for measuring the pH.

Desipramine and all the available reagents used were of analytical grade. We chose Merck (Darmstadt: Germany) for purchasing the reagents. Thus, in order to procure the buffers, we applied the *ortho*-phosphoric acid and the respective salts for providing pH ranges between 2.0 and 9.0.

Preparation of magnetic iron oxide-supported copper oxide NPs (Fe_3O_4/CuO)

First, the magnetic NP of Fe_3O_4 was synthesized by an easy coprecipitation modified technique[45] using a solution of $FeCl_2 \cdot 4H_2O$ (10 mmol) and $FeCl_3 \cdot 6H_2O$ (20 mmol) in 120 mL deionized water, and the solution was placed under nitrogen gas. The solution was stirred for 30 minutes, and at this time, 10 mL of NH_4OH (8 M) was added drop by drop into the solution. The black resulting solids were separated by an exterior

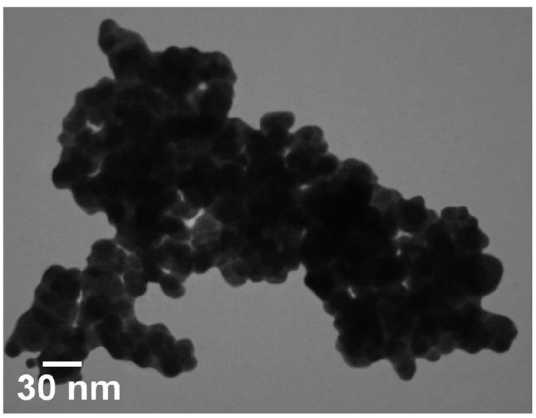

Fig. 1 The TEM image of magnetic Fe_3O_4/CuO.

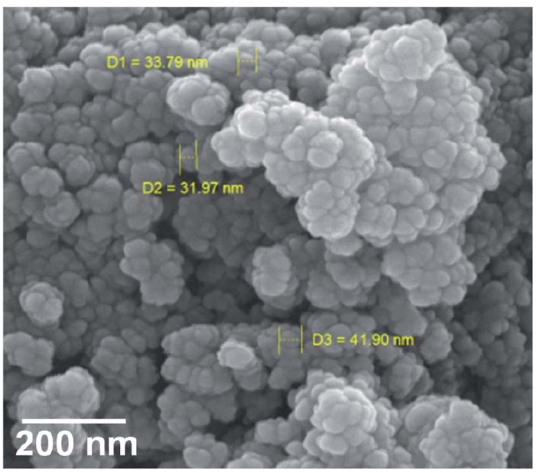

Fig. 2 The SEM image of magnetic Fe_3O_4/CuO.

magnetic field. Subsequently, the deionized water was used to wash it numerous times and dried for 4 h at 80 °C (eqn (1)).

$$2Fe^{3+} + Fe^{2+} + 8OH^- \rightarrow Fe_3O_4 + 4H_2O \quad (1)$$

In the second section of this work, we synthesized magnetic iron oxide-supported copper oxide NPs using the layer to layer method. 0.5 g of nano-sized Fe_3O_4 was added to 25 mL of thioglycolic acid (10 mM) under shaking for 1 h at room temperature. Then, the product was gathered by an exterior magnetic field, followed by washing the product with ethanol and deionized water two times. The functionalized Fe_3O_4 core, synthesized as described above, was then dispersed in 45 mL of $Cu(NO_3)_2$ (10 mM) for 20 minutes under ultrasonication until a uniform solution was obtained. Then, the precipitate obtained was collected with an external magnetic field and was washed two times by ethanol. To the obtained and washed precipitates, 25 mL of thioglycolic acid solution (10 mM) was added and stirred for 30 minutes at 60 °C. Then, the magnetic particles were isolated with an exterior magnetic field and were washed with ethanol. These cycles were repeated for 30 times, and then the samples were washed two times with ethanol, with the finally obtained sample being dried under vacuum for 6 h at 170 °C.

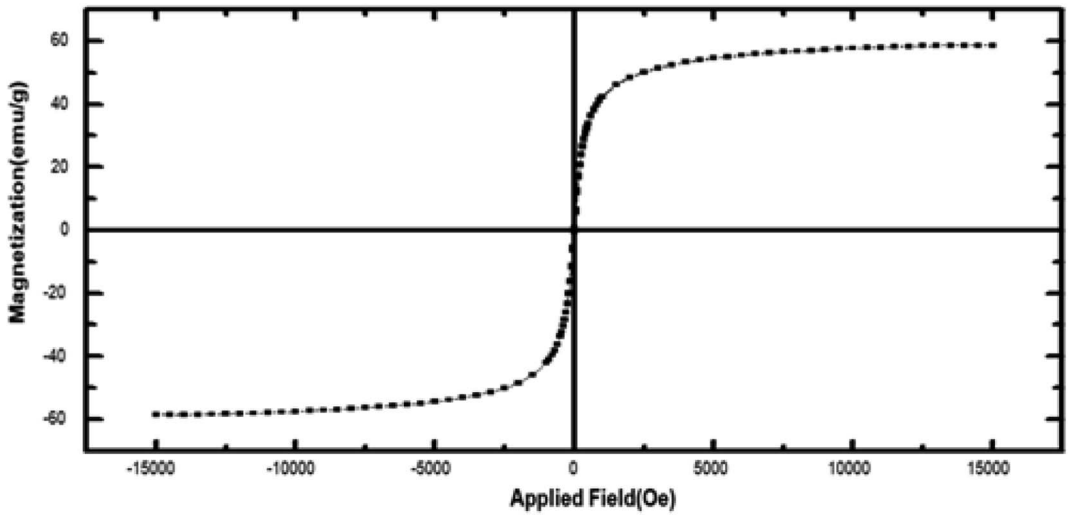

Fig. 3 The VSM spectrum of magnetic Fe_3O_4/CuO.

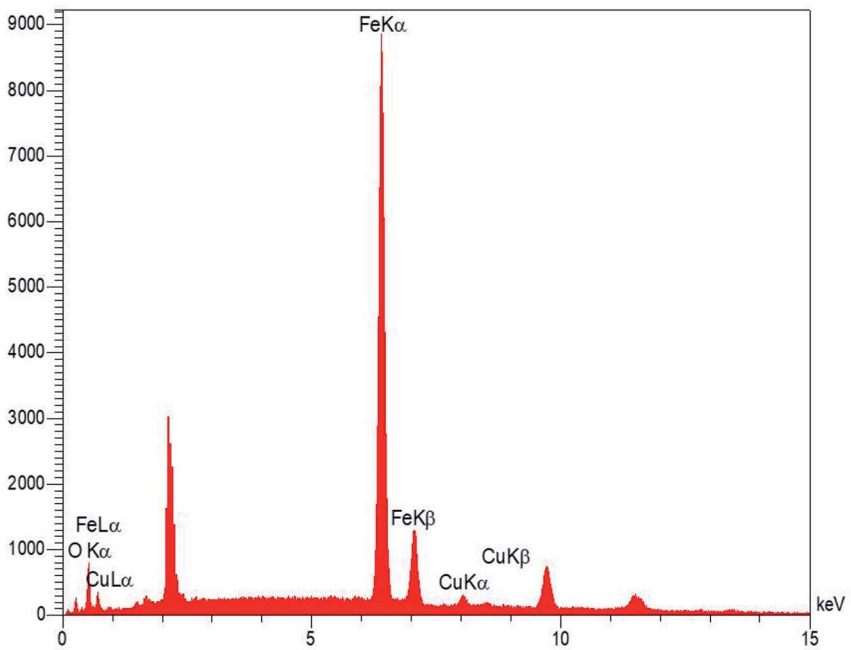

Fig. 4 The EDS image of magnetic Fe_3O_4/CuO.

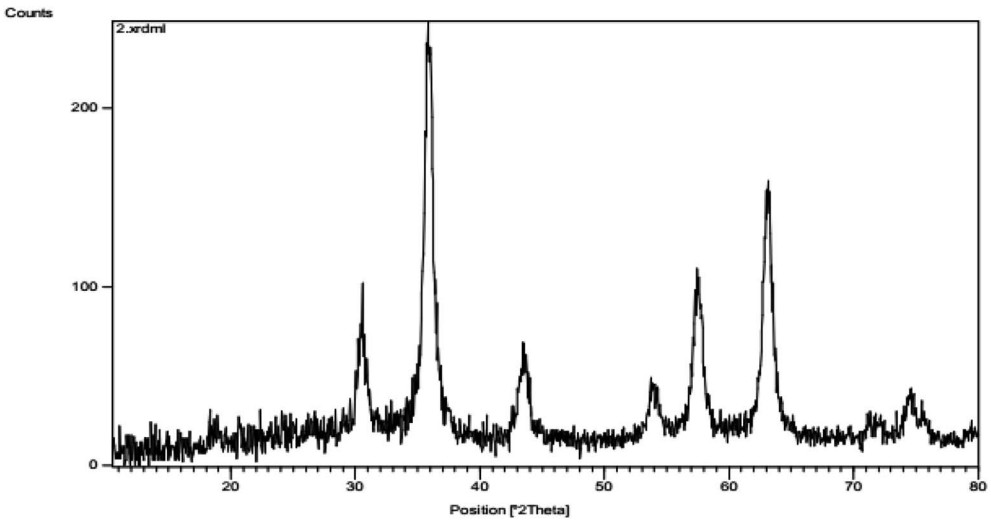

Fig. 5 The XRD pattern of magnetic Fe_3O_4/CuO.

Preparing the electrode

Based on the easy process presented below, the bare SPE was coated. 1 mg of Fe_3O_4/CuO NPs was dispersed in 1 mL of an aqueous solution *via* ultra-sonication with an interval of 45 minutes. Afterward, 3 μL of the procured suspension was dropped onto the carbon working electrode surface. Finally, it was dried at room temperature.

Preparation of real samples

Desipramine tablets (Ruzdarou, Iran [labelled value desipramine = 25 mgper tablet]) were purchased. The desipramine pills were thoroughly powdered and homogenized prior to the preparation of 20 mL of the 0.1 M stock solution. In fact, we sonicated the solution for assuring an ideal dissolution. Then, we filtered the solution. Afterward, we poured the determined volume of the transparent filtrate into the electrochemical cell consisting of 10 mL of 0.1 M PBS (pH = 7) for recording the DPV voltammogram.

In addition, we kept the urine specimens inside a refrigerator immediately after being collected. Then, 10 mL of the specimens was centrifuged at 2000 rpm for fifteen minutes. In the next stage, we filtered the supernatant through a 0.45 μm filter. Afterward, distinct contents of the solution were transported into a 25 mL volumetric flask, and the solution was diluted to the mark with PBS (pH = 7.0). Then, diverse amounts of desipramine were used to spike the diluted urine specimens.

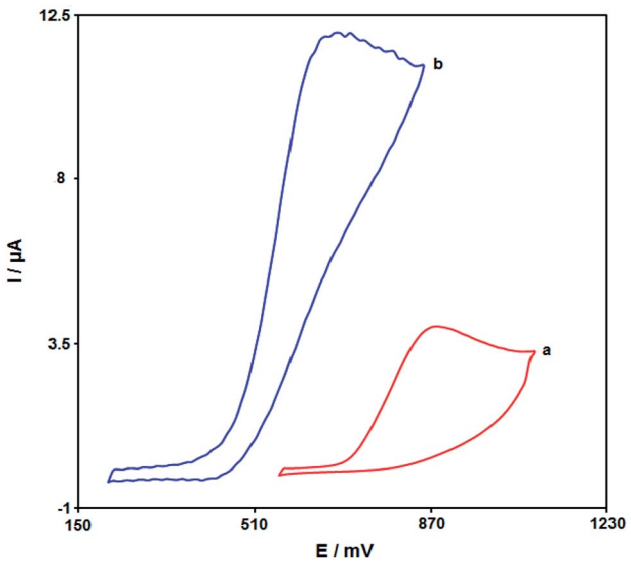

Fig. 6 The cyclic voltammogram of (a) bare SPE and (b) Fe_3O_4/CuO/SPE in 0.1 M PBS (pH = 7.0) in the presence of 100.0 μM desipramine at the scan rate of 50 mV s^{-1}.

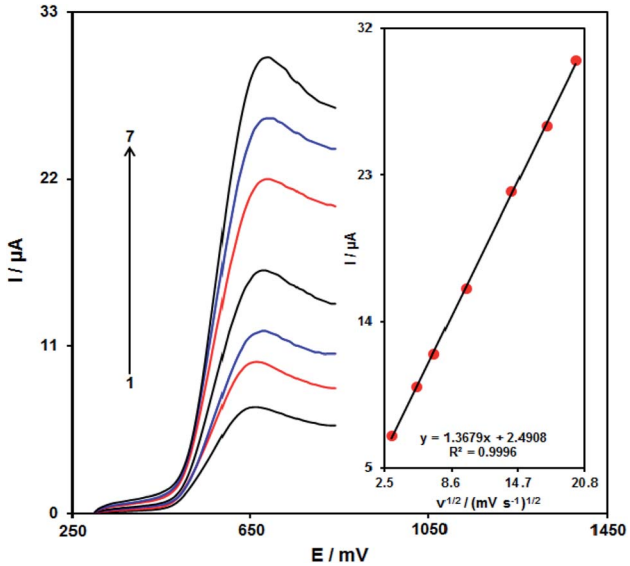

Fig. 7 Linear sweep voltammogram of Fe_3O_4/CuO/SPE in 0.1 M PBS (pH = 7.0) consisting of 100.0 μM desipramine at diverse scan rates. Numbering 1–7 refer to 10, 30, 50, 100, 200, 300, and 400 mV s^{-1}, respectively. Inset: variation of anodic peak current *vs.* $\nu^{1/2}$.

Finally, desipramine contents were examined by our technique *via* the standard addition procedure.

Electrochemical measurements

Desipramine detection was performed using the CV and DPV methods, with a potentiostat/galvanostat Autolab PGSTAT 302N with GPES software. A graphite electrode (modified with magnetic iron oxide-supported copper oxide NPs (Fe_3O_4/CuO)) was used as the working electrode, together with a graphite counter electrode, and a silver pseudo-reference electrode. CV and DPV were carried out by repeated potential scanning in the range of 0.34 to 0.98 V at a scan rate of 50 mV s^{-1} in the presence of different concentrations of desipramine (0.08–400.0 μM) dissolved in 0.1 M PBS pH = 7.0. All electrochemical measurements were carried out at room temperature.

Results and discussion

Morphology and structure of magnetic Fe_3O_4/CuO

Fig. 1 shows magnetic Fe_3O_4/CuO, which were characterized by TEM. Fig. 2 shows the spherical morphology for this compound obtained by SEM. Fig. 3 shows the magnetic measurements of magnetic Fe_3O_4/CuO at room temperature. Due to the hysteresis loops, the saturation magnetization (MS) was found to be 60 emu g^{-1} for the above compound. Fig. 4 shows the EDX analyses of the as-synthesized NPs, which depicts the presence of the Fe, Cu, and O elements in this figure, clearly indicating the purity of the as-synthesized NPs.

The XRD pattern in Fig. 5 confirmed the successful synthesis of the magnetic Fe_3O_4/CuO matched with the reference code: 00-025-0283 of the $CuFe_2O_4$ copper spinel form. By using the Scherer equation and 2θ, the mean size of the grain size for the magnetic Fe_3O_4/CuO (12 nm) can be obtained. Peaks for this compound were observed at 2θ = 18.64(111), 30.50(220), 35.89(400), 43.52(311), 53.97(511), 57.46(440), 63.11(533), and 71.70(444) planes, as shown in Fig. 5.[46,47]

Electro-chemical behavior of desipramine on the Fe_3O_4/CuO/SPE

An optimum pH-value is required for studying the electrochemical behaviour of desipramine, which is pH-dependent so that we can obtain a specific output. However, we conducted the tests by employing the modified electrodes at distinct pH-values in the range between 2.0 and 9.0, with the occurrence of the

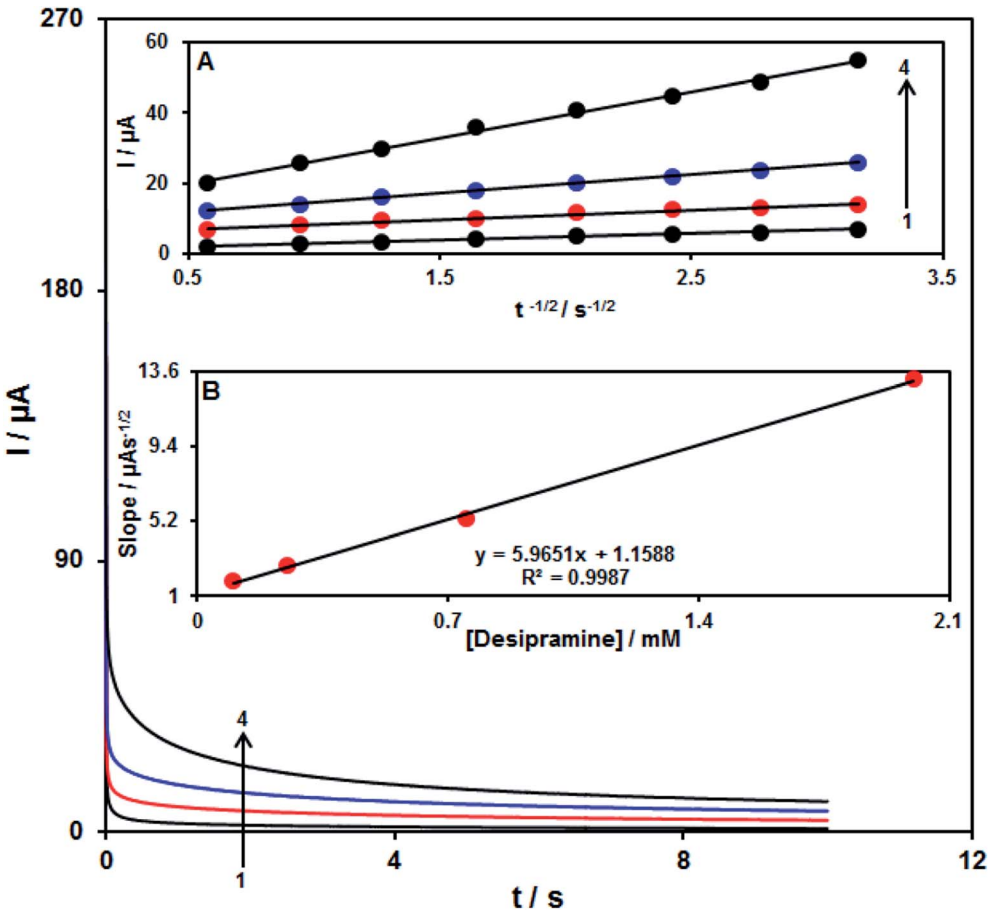

Fig. 8 Chrono-amperograms achieved at Fe_3O_4/CuO/SPE in 0.1 M PBS (pH = 7.0) for distinct concentration of desipramine. Numbering 1–4 refer to 0.1, 0.25, 0.75, and 2.0 mM of desipramine, respectively. Insets: (A) *I* plot *vs.* $t^{-1/2}$ achieved from chrono-amperograms 1 to 4. (B) The slope plot of straight lines *versus* desipramine concentration.

most acceptable outputs for desipramine electro-oxidation at pH equal to 7.0.

Fig. 6 portrays the final cyclic voltammogram in the presence of 100.0 μM desipramine through the bare SPE (Curve a) and the Fe_3O_4/CuO/SPE (Curve b). As seen from the CV outputs, the greatest level of desipramine oxidation on the Fe_3O_4/CuO/SPE occurs at 670 mV, which is nearly 110 mV more negative in comparison to the unmodified SPE.

Effects of the scan rate on the outputs

It is notable that the enhancement of the scan rate causes greater oxidation peak currents with regard to the outputs gained by examining the effects of the potential scan rates on desipramine oxidation current (Fig. 7). In addition, we found a linear association between Ip and the square root of the potential scan rate ($v^{1/2}$), indicating that diffusion controls the desipramine oxidation process.

Chronoamperometric analysis

Analysis of chrono-amperometry for desipramine samples was done using the Fe_3O_4/CuO/SPE at 0.72 V. Fig. 8 represents the chronoamperometric results of the distinct concentrations of desipramine samples in PBS (pH = 7.0). Here, the Cottrell equation for analysing the chronoamperometry of the electro-active moiety under the mass transfer-limited condition will be presented as

$$I = nFAD^{1/2}C_b\pi^{-1/2}t^{-1/2}$$

where D refers to the diffusion coefficient ($cm^2\ s^{-1}$), and C_b is the applied bulk concentration (mol cm^{-3}). Fig. 8A depicts the experimental outputs of I *versus* $t^{-1/2}$ so that the best fits were obtained for distinct concentrations of desipramine. Moreover, Fig. 8B is a representation of the resultant slopes relative to the straight line in Fig. 8A *versus* desipramine concentration. In addition, the mean value of D was calculated to be 3.0×10^{-6} $cm^2\ s^{-1}$ based on the Cottrell equation and the final slope.

Calibration curve

With regard to the desipramine resultant peak currents through Fe_3O_4/CuO/SPE, desipramine was quantitatively analyzed in the water solution (Fig. 9). We also utilized the modified electrode (Fe_3O_4/CuO/SPE) as the working electrode within a range of desipramine. DPV, because of its benefits like greater sensitivity and more reasonable functions in the analytical utilizations, was used. However, the outputs implied the linear relationship between the peak current and desipramine concentrations in the concentration range between 0.08 and 400.0 μM. Finally, LOD was calculated to be 0.03 μM. These values were

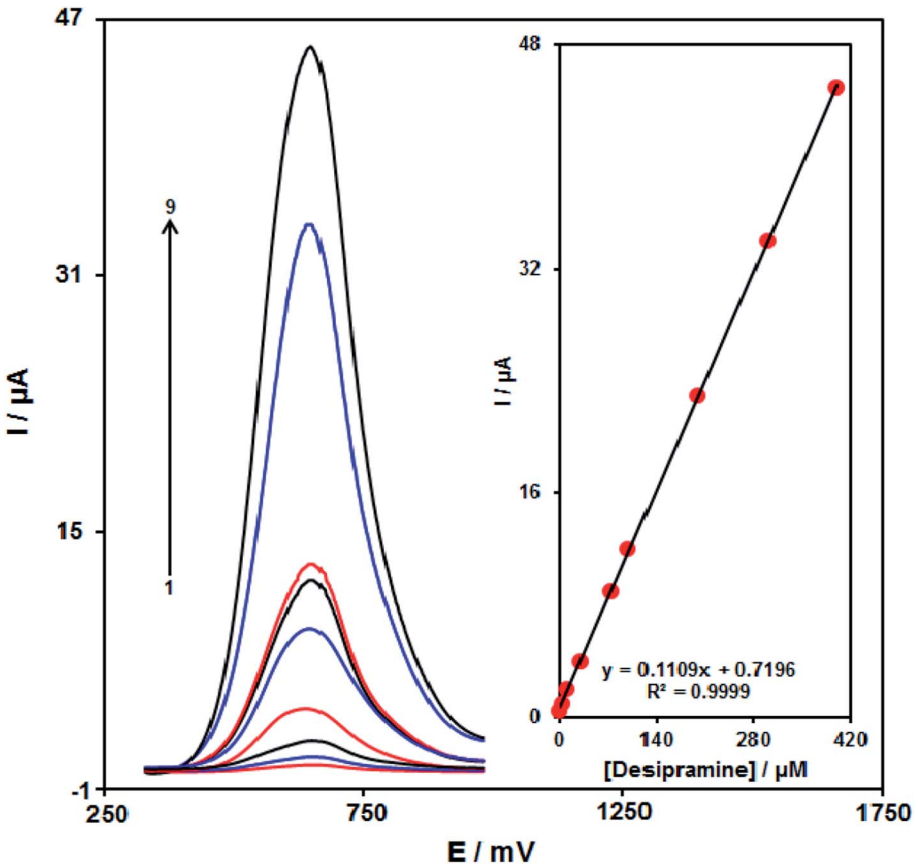

Fig. 9 Differential pulse voltammograms of Fe_3O_4/CuO/SPE in 0.1 M PBS (pH = 7.0) consisting of distinct concentrations of desipramine. Numbering 1–9 refer to 0.08, 3.0, 10.0, 30.0, 75.0, 100.0, 200.0, 300.0, and 400.0 μM of desipramine, respectively. Inset: the peak current plot as a function of desipramine concentrations ranging between 0.08 and 400.0 μM.

Table 1 Comparison of the efficiency of some methods used in the detection of desipramine

Method	Modifier	LOD	LDR	Ref.
High performance liquid chromatography	—	1.0 ng ml	15.0–400.0 ng ml	41
High performance liquid chromatography	—	0.03 μg L^{-1}	0.05–0.684 μg L^{-1}	48
Voltammetry	Reduced graphene oxide	1.04 nM	0.3–2.5 μM	49
Voltammetry	Poly(methyl methacrylate)	—	0.01–0.1 μM	50
Potentiometry	*N*-(1-Naphthyl)ethylenediamine dihydrochloride-tetraphenyl borate	0.09	1–10 000	51
Voltammetry	Fe_3O_4/CuO NPs	0.03 μM	0.08–400.0 μM	This work

comparable to the values reported by other research groups for the determination of desipramine (Table 1). As can be seen in some cases that the linear dynamic range in the case of our method was better than other cases, and in some cases, the detection limit of our work was better than other works.

Generalizability and stability of Fe_3O_4/CuO/SPE

We kept our sensor at pH equal to 7.0 in PBS for 17 days in order to test the Fe_3O_4/CuO/SPE stability. Afterward, we recorded the cyclic voltammogram of the solution consisting of 35.0 μM of desipramine in order to compare it with the cyclic voltammogram achieved prior to immerging. According to the analyses, the desipramine oxidation peak did not change, and the current exhibited ~2.2% reduction in the signals as compared with the early responses, proposing that Fe_3O_4/CuO/SPE enjoys acceptable stability.

It is notable that the CV was used to determine the antifouling property of the modified SPE towards the oxidation of desipramine and their products for the modified SPE prior to and following the utilization in the presence of desipramine. In addition, we registered the cyclic voltammograms in the presence of desipramine after 15 times cycling of potential of 50 mV s^{-1}. The analysis showed a decline in the currents by ~2.1%, with no alteration in the peak potential.

Analysis of real samples

We used desipramine in the desipramine tablet and the urine samples *via* the above procedure in order to assess the proposed modified electrode utility to detect the real samples. Therefore, the standard addition procedure was utilized. Table 2 reports the analysis outputs. Correspondingly, the outputs obtained for desipramine recovery were very good so that they could be generalized using the mean relative standard deviation.

Table 2 The application of Fe_3O_4/CuO/SPE for the determination of desipramine in desipramine tablet and urine samples (n = 5). All concentrations are in μM

Sample	Spiked	Found	Recovery (%)	R.S.D. (%)
Desipramine tablet	0	4.5	—	3.1
	3.0	7.7	102.7	2.4
	8.0	12.4	99.2	2.9
	13.0	17.6	100.6	3.1
	18.0	22.2	98.7	1.8
Urine	—	—	—	—
	6.0	5.9	98.3	2.7
	12.0	12.3	102.5	3.5
	18.0	17.5	97.2	1.9
	24.0	24.3	101.2	2.8

Conclusions

In this report, Fe_3O_4/CuO was procured by a coprecipitation procedure. Moreover, the Fe_3O_4/CuO generation was confirmed by the EDS analysis, XRD, SEM, TEM, and VSM. Further, the as-prepared Fe_3O_4/CuO/SPE was followed by reasonable electrocatalytic abilities to detect desipramine. Based on the results, our new Fe_3O_4/CuO/SPE sensor possesses very good analytical functions with multiple beneficial features, like a wider linear range (0.08–400.0 μM), low limit of detection (0.03 μM), better storage, and stability. Additionally, the urine specimen and desipramine tablet were used to assess the functional utility of the sensor, which shows very acceptable results and make Fe_3O_4/CuO one of the hopeful electrocatalysts to detect desipramine in the drug and biological specimens.

Conflicts of interest

All the authors declare no conflict of interest.

Acknowledgements

The authors acknowledge the financial support provided for this project (Project No. 98000791) by Neuroscience Research Center, Kerman University of Medical Sciences, Kerman, Iran. This research was supported by the Future Material Discovery Program (2016M3D1A1027666), Basic Science Research Program (2017R1A2B3009135) through the National Research Foundation of Korea, and China Scholarship Council (201808260042) is appreciated.

References

1 M. Mazloum-Ardakani, H. Beitollahi, M. K. Amini, F. Mirkhalaf, B. F. Mirjalili and A. Akbari, *Analyst*, 2011, **136**, 1965–1970.
2 X. Yang, M. Gao, H. Hu and H. Zhang, *Phytochem. Anal.*, 2011, **22**, 291–295.
3 N. Rabiee, M. Safarkhani and M. Rabiee, *Asian J. Nanosci. Mater.*, 2018, **1**, 63–73.

4 H. Karimi-Maleh and O. A. Arotiba, *J. Colloid Interface Sci.*, 2020, **560**, 208–212.
5 D. Sun, F. Wang, K. Wu, J. Chen and Y. Zhou, *Microchim. Acta*, 2009, **167**, 35–39.
6 J. B. Raoof, N. Teymoori, M. A. Khalilzadeh and R. Ojani, *Mater. Sci. Eng., C*, 2015, **47**, 77–84.
7 M. A. Khalilzadeh, S. Tajik, H. Beitollahi and R. A. Venditti, *Ind. Eng. Chem. Res.*, 2020, **59**, 4219–4228.
8 M. A. Khalilzadeh and M. Borzoo, *J. Food Drug Anal.*, 2016, **24**, 796–803.
9 W. H. Elobeid and A. A. Elbashir, *Prog. Chem. Biochem. Res.*, 2019, **2**, 24–33.
10 H. Beitollahi, S. Tajik, M. H. Asadi and P. Biparva, *J. Anal. Sci. Technol.*, 2014, **5**, 1–9.
11 M. Portaccio, D. Di Tuoro, F. Arduini, D. Moscone, M. Cammarota, D. G. Mita and M. Lepore, *Electrochim. Acta*, 2013, **109**, 340–347.
12 M. Payehghadr, S. Adineh Salarvand, F. Nourifard, M. K. Rofouei and N. Bahramipanah, *Adv. J. Chem., Sect. A*, 2019, **2**, 377–385.
13 H. Karimi-Maleh, C. T. Fakude, N. Mabuba, G. M. Peleyeju and O. A. Arotiba, *J. Colloid Interface Sci.*, 2019, **554**, 603–610.
14 C. Rajkumar, B. Thirumalraj, S. M. Chen and S. Palanisamy, *RSC Adv.*, 2016, **6**, 68798–68805.
15 S. Tajik, M. A. Taher, H. Beitollahi and M. Torkzadeh-Mahani, *Talanta*, 2015, **134**, 60–64.
16 *Nanomaterials and Nanochemistry*, ed. C.B. Echignac, P. Houdy and M. Lahmani, Springer-Verlag, Berlin, Heidelberg, 2007.
17 H. Karimi-Maleh, P. Biparva and M. Hatami, *Biosens. Bioelectron.*, 2013, **48**, 270–275.
18 Y. Su, Y. Xie, X. Hou and Y. Lv, *Appl. Spectrosc. Rev.*, 2014, **49**, 201–232.
19 P. Biparva, S. M. Abedirad and S. Y. Kazemi, *Talanta*, 2014, **130**, 116–121.
20 H. Beitollahi, M. A. Khalilzadeh, S. Tajik, M. Safaei, K. Zhang, H. W. Jang and M. Shokouhimehr, *ACS Omega*, 2020, **5**, 2049–2059.
21 S. Tajik, H. Beitollahi and P. Biparva, *J. Serb. Chem. Soc.*, 2018, **83**, 863–874.
22 H. Beitollahi, M. Safaei and S. Tajik, *Electroanalysis*, 2019, **31**, 1135–1140.
23 H. Karimi-Maleh, C. T. Fakude, N. Mabuba, G. M. Peleyeju and O. A. Arotiba, *J. Colloid Interface Sci.*, 2019, **554**, 603–610.
24 H. Ibrahim, Y. Temerk and N. Farhan, *RSC Adv.*, 2016, **6**, 90220–90231.
25 H. Beitollahi, H. Karimi-Maleh and H. Khabazzadeh, *Anal. Chem.*, 2008, **80**, 9848–9851.
26 T. Pagar, S. Ghotekar, K. Pagar, S. Pansambal and R. Oza, *J. Chem. Rev.*, 2019, **1**, 260–270.
27 M. M. Motaghi, H. Beitollahi, S. Tajik and R. Hosseinzadeh, *Int. J. Electrochem. Sci.*, 2016, **11**, 7849–7860.
28 B. Fang, G. Wang, W. Zhang, M. Li and X. Kan, *Electroanalysis*, 2005, **17**, 744–748.
29 H. Yin, Y. Zhou, X. Meng, T. Tang, S. Ai and L. Zhu, *Food Chem.*, 2011, **127**, 1348–1353.
30 L. Yang, X. Ren, F. Tang and L. Zhang, *Biosens. Bioelectron.*, 2009, **25**, 889–895.
31 J. Qiu, H. Peng and R. Liang, *Electrochem. Commun.*, 2007, **9**, 2734–2738.
32 C. Yu, J. Guo and H. Gu, *Electroanalysis*, 2010, **22**, 1005–1011.
33 H. Beitollahi, H. Mahmoudi-Moghaddam and S. Tajik, *Anal. Lett.*, 2019, **52**, 1432–1444.
34 T. Dayakar, K. V. Rao, K. Bikshalu, V. Malapati and K. K. Sadasivuni, *Biosens. Bioelectron.*, 2018, **111**, 166–173.
35 B. Pérez-Fernández, D. Martín-Yerga and A. Costa-García, *RSC Adv.*, 2016, **6**, 83748–83757.
36 M. Khairy, H. A. Ayoub and C. E. Banks, *Food Chem.*, 2018, **255**, 104–111.
37 M. R. Ganjali, Z. Dourandish, H. Beitollahi, S. Tajik, L. Hajiaghababaei and B. Larijani, *Int. J. Electrochem. Sci.*, 2018, **13**, 2448–2461.
38 P. Knihnicki, M. Wieczorek, M. Bienias, R. Wietecha-Posłuszny, M. Woźniakiewicz and P. Kościelniak, *Procedia Eng.*, 2012, **47**, 1342.
39 M. W. Linder and P. E. Keck, Standards of laboratory practice: antidepressant drug monitoring, *Clin. Chem.*, 1998, **44**, 1073–1084.
40 G. Sahin, B. Giray and P. Erkekoglu, *Turk. Klin. Tip Bilimleri Derg.*, 2008, **28**, 533–540.
41 A. Onal and A. Oztunc, *Rev. Anal. Chem.*, 2011, **30**, 165–171.
42 R. de la Torre, J. Ortuno, J. A. Pascual, S. Gonzalez and J. Ballesta, *Ther. Drug Monit.*, 1998, **20**, 340–346.
43 M. I. Acedo-Valenzuela, N. Mora-Diez, T. Galeano-Diaz and A. Silva-Rodriguez, *Anal. Sci.*, 2010, **26**, 699–702.
44 H. N. Deepakumari, M. K. Prashanth, B. C. V. Kumar and H. D. Revanasiddappa, *J. Appl. Spectrosc.*, 2015, **81**, 1004–1011.
45 Y. Wei, B. Han, X. Hu, Y. Lin, X. Wang and X. Deng, *Procedia Eng.*, 2012, **27**, 632–637.
46 P. Scherrer, *Göttinger Nachrichten Gesell.*, 1918, **2**, 98–100.
47 A. Patterson, *Phys. Rev.*, 1939, **56**, 978–982.
48 M. Wozniakiewicz, J. Kuczara and P. Koscielniak, *Probl. Forensic Sci.*, 2007, **69**, 90–97.
49 F. H. Cincotto, D. L. C. Golinelli, S. A. S. Machado and F. C. Moraes, *Sens. Actuators, B*, 2017, **239**, 488–493.
50 P. Knihnicki, M. Wieczorek, A. Moos, P. Kościelniak, R. Wietecha-Posłuszny and M. Woźniakiewicz, *Sens. Actuators, B*, 2013, **189**, 37–42.
51 A. A. Ensafi and A. R. Allafchian, *IEEE Sens. J.*, 2011, **11**, 2576–2582.

